CALPHAD: Computer Coupling of Phase Diagrams and Thermochemistry 35 (2011) 473–478

Contents lists available at SciVerse ScienceDirect

CALPHAD: Computer Coupling of Phase Diagrams and Thermochemistry

journal homepage: www.elsevier.com/locate/calphad

Thermodynamic assessments of the Er–Sb and Sb–Tm systems

S.L. Wang [a], Z.B. Hu [a], F. Gao [b], C.P. Wang [c], X.J. Liu [c,*]

[a] College of Chemistry and Materials Science, Longyan University, Longyan, 364000, PR China

[b] College of Materials Science and Engineering, Qingdao University of Science and Technology, Qingdao, 266042, PR China

[c] Department of Materials Science and Engineering, College of Materials, Xiamen University, Xiamen, 361005, PR China

ARTICLE INFO

Article history:
Received 29 April 2011
Received in revised form
25 July 2011
Accepted 4 August 2011
Available online 1 September 2011

Keywords:
CALPHAD
Er–Sb system
Sb–Tm system
Phase diagram

ABSTRACT

By using the calculation of phase diagrams (CALPHAD) method, thermodynamic assessments of the Er–Sb and Sb–Tm systems were carried out based on the available experimental data including thermodynamic properties and phase equilibria. The Gibbs free energies of the liquid, hcp, and rhombohedral phases in the Er–Sb and Sb–Tm systems were modeled by the substitutional solution model with the Redlich–Kister formula, and the intermetallic compounds (Er_5Sb_3, αErSb, βErSb, $ErSb_2$, Sb_2Tm, αSbTm, βSbTm, αSb_3Tm_5, and βSb_3Tm_5 phases) in these two binary systems were described by the sublattice model. An agreement between the present calculated results and experimental data was obtained.

1. Introduction

Magnesium (Mg) alloys have been widely used in many industrial fields due to their superior characteristics such as low density, high specific strength, and good castability [1]. The addition of rare earth (RE) elements to Mg base alloys can enhance the high-temperature properties, corrosion resistance and casting characteristics [2,3]. When Sb and RE atoms coexist in Mg base alloys, Sb will combine with the RE to form dispersed particles, which are mainly intermetallic compound phase distributed at the grain boundaries and which improve the high-temperature properties of the Mg base alloys [4]. Therefore, it is important to understand the phase equilibria in Sb–RE binary systems.

The CALPHAD method, which is a powerful tool to reduce the cost and time during development of materials, effectively provides a clear guideline for material design. In order to design high-performance alloys with rare earth elements, it is important to develop a thermodynamic database including rare earth element alloys. Currently, our group is focusing on the development of a thermodynamic database of rare earth alloy systems, which is important for the design of alloys with additions of rare earth elements. As part of this thermodynamic database, this work presents the thermodynamic descriptions of the Er–Sb and Sb–Tm binary systems based on the available experimental data by means of the CALPHAD method.

2. Experimental information

2.1. The Er–Sb system

The Er–Sb system consists of two terminal solution phases (hcp (Er) and rhombohedral (Sb) phases) and four intermetallic compounds (Er_5Sb_3, αErSb, βErSb, and $ErSb_2$ phases). Abdusalyamova et al. [5] were the first to report incongruent melting of the $ErSb_2$ phase at 650 °C by means of differential thermal analysis (DTA). Later, based on thermal, microstructural, and X-ray diffraction analysis, Abdusalyamova [6] investigated the phase diagram in the Er–Sb system, and reported three stoichiometric compounds: Er_5Sb_3 (peritectic formation at 1640 °C), ErSb (melting point 2040 °C), and $ErSb_2$ (peritectic formation at 650 °C). A reversible polymorphic transition (αErSb $\leftrightarrow$ βErSb at 1810 °C) was observed by Abdusalyamova [6]. According to the work of Refs. [5,6], Okamoto [7] compiled the phase diagram of the Er–Sb system, which is shown in Fig. 1. Using high-temperature DTA, X-ray diffraction, and microstructural methods of analysis, Abdusalyamova and Rachmatov [8,9] studied the phase diagram in the Er–Sb system and determined two eutectic reactions: L ($\sim$15.5 at.% Sb) $\leftrightarrow$ (Er) + Er_5Sb_3 at 1170 °C, and L($\sim$99 at.% Sb) $\leftrightarrow$ $ErSb_2$ + (Sb) at 625 °C [8](L(99.4 at.% Sb) $\leftrightarrow$ $ErSb_2$ + (Sb) at 620 °C [9]). In the work of Abdusalyamova and Rachmatov [8,9], the maximum solid solubility of Sb in the hcp (Er) phase was indicated to be greater than 1 at.%.

In addition, using a direct-reaction calorimeter, Pratt and Chua [10] reported the standard enthalpy of formation of the αErSb phase. Goryacheva et al. [11] extrapolated the standard enthalpies

* Corresponding author. Tel.: +86 592 2187888; fax: +86 592 2187966.
E-mail address: lxj@xmu.edu.cn (X.J. Liu).

0364-5916/$ – see front matter © 2011 Published by Elsevier Ltd
doi:10.1016/j.calphad.2011.08.001

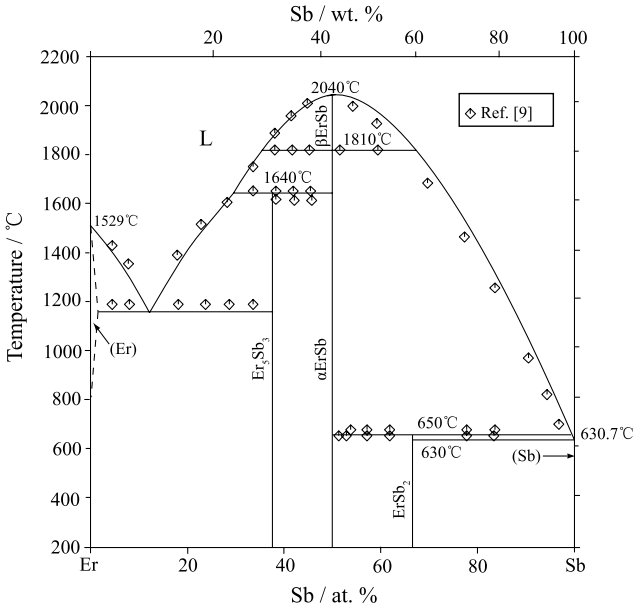

Fig. 1. The phase diagram of the Er–Sb system reviewed by Okamoto [7].

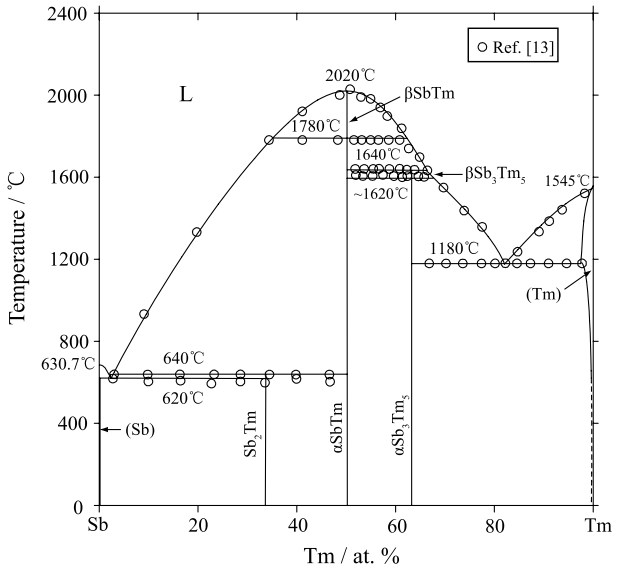

Fig. 2. The phase diagram of the Sb–Tm system reviewed by Okamoto [14].

and entropies of formation of the αErSb and $ErSb_2$ phases by the electromotive force (EMF) method. Using Miedema's model, Colinet et al. [12] predicted that the value of the enthalpy of mixing of the liquid phase with the reference states of pure liquid metals at 50 at.% Sb in the Er–Sb system is −53 kJ/mol; however, no temperature dependence was given in the work of Colinet et al. [12].

2.2. The Sb–Tm system

The Sb–Tm system consists of two terminal solution phases (rhombohedral (Sb) and hcp (Tm) phases) and five intermetallic compounds (Sb_2Tm, αSbTm, βSbTm, αSb_3Tm_5, and βSb_3Tm_5 phases). Abdusalyamova et al. [5] were the first to report incongruent melting of the $SbTm_2$ phase at 640 °C by means of DTA. Later, based on different thermal and X-ray phase and microstructural analyses, Abdusalyamova et al. [13] investigated the phase diagram in the Sb–Tm system, and reported three stoichiometric compounds: $SbTm_2$ (peritectic formation at 640 °C), SbTm (melting point 2020 °C), and Sb_5Tm_3 (peritectic formation at 1640 °C). Abdusalyamova et al. [13] also determined two eutectic reactions: $L(<1.0$ at.% Tm) $\leftrightarrow Sb_2Tm + (Sb)$ at 620 °C, and $L(85$ at.% Tm) $\leftrightarrow Sb_3Tm_5 + (Tm)$ at 1180 °C. Two reversible polymorphic transitions (αSbTm $\leftrightarrow$ β SbTm at 1780 °C and αSb_3Tm_5 $\leftrightarrow$ βSb_3Tm_5 at ∼ 1620 °C) were observed by Abdusalyamova et al. [13]. In the work of Abdusalyamova et al. [13], the maximum solid solubility of Sb in the hcp (Tm) phase was suggested to be less than 1.5 at%. The phase diagram of the Sb–Tm system was reviewed by Okamoto [14], and is shown in Fig. 2.

In addition, using a direct-reaction calorimeter, Pratt and Chua [10] reported the standard enthalpy of formation of the αSbTm phase. Boer et al. [15] reported the calculated standard enthalpies of formation of the SbTm phase by using Miedema's model. Using the same method, Colinet et al. [12] predicted the standard enthalpies of formation of the Sb_2Tm, αSbTm, and α Sb_3Tm_5 phases. Colinet et al. [12] also predicted that the value of the enthalpy of mixing of the liquid phase with the reference states of pure liquid metals at 50 at% Tm in the Sb–Tm system is −52 kJ/mol; however, no temperature dependence was given in the work of Colinet et al. [12].

3. Thermodynamic models

3.1. Solution phases

In the Er–Sb and Sb–Tm binary systems (which are both binary A–B systems), the liquid, hcp, and rhombohedral phases are described as disordered substitutional solutions. The Gibbs free energies of the liquid, hcp, and rhombohedral phases are described by the substitutional solution model, as follows:

$$G_m^{\phi} = \sum_{i=\mathrm{A,B}} {}^0G_i^{\phi} x_i + RT \sum_{i=\mathrm{A,B}} x_i \ln x_i + \Delta^E G_m^{\phi}, \tag{1}$$

where ${}^0G_i^{\phi}$ is the Gibbs free energy of the pure component i in the respective reference state with phase ϕ, which is taken from the SGTE pure element database [16]; x_i denotes the mole fraction of component i; R is the gas constant; T is the absolute temperature; and the term $\Delta^E G_m^{\phi}$ represents the excess Gibbs free energy, which is expressed in Redlich–Kister polynomial form [17] as

$$\Delta^E G_m^{\phi} = x_\mathrm{A} X_\mathrm{B} \sum_{m=0}^{n} {}^mL_{\mathrm{A,B}}^{\phi} (x_\mathrm{A} - x_\mathrm{B})^m, \tag{2}$$

$${}^mL_{\mathrm{A,B}}^{\phi} = a + bT, \tag{3}$$

where ${}^mL_{\mathrm{A,B}}^{\phi}$ is the binary interaction parameter, and the coefficients of a and b are evaluated on the basis of available experimental data.

3.2. Stoichiometric intermetallic compounds

All the intermetallic compounds in the Er–Sb and Sb–Tm binary systems are treated as stoichiometric phases. Due to lack of the heat capacity data and according to the Neumann–Koppe rule, the Gibbs free energy per mole of formula unit A_pB_q can be expressed as follows:

$$\Delta^0 G_f^{\mathrm{A}_p\mathrm{B}_q} = G_{\mathrm{A:B}}^{\mathrm{A}_p\mathrm{B}_q} - p^0G_\mathrm{A}^{SER} - q^0G_\mathrm{B}^{SER} = a' + b'T, \tag{4}$$

where $\Delta^0 G_f^{\mathrm{A}_p\mathrm{B}_q}$ indicates the standard Gibbs free energy of formation of the stoichiometric compound from pure elements; the parameters of a' and b' are evaluated in the present work.

Table 1
Experimental and calculated invariant reactions in the Er–Sb system.

Invariant reaction	Reaction type	Composition (at% Sb)			Temperature (°C)	Reference
$L \leftrightarrow (Er) + Er_5Sb_3$	Eutectic	~15.5	>1.0	25	1170	[8,9]
		13.2	1.4	25	1170.1	This work
$L + \alpha ErSb \leftrightarrow Er_5Sb_3$	Peritectic		50.0	37.5	1640	[6,8,9]
		29.9	50.0	37.5	1639.8	This work
$\alpha ErSb \leftrightarrow \beta ErSb$	Polymorphic		50.0		1810	[6,8,9]
			50.0		1810.1	This work
$L \leftrightarrow \beta ErSb$	Congruent		50.0		2040	[6,8,9]
			50.0		2040	This work
$L + \alpha ErSb \leftrightarrow ErSb_2$	Peritectic		50.0	66.7	650	[5,6,8,9]
		98.7	50.0	66.7	650	This work
$L \leftrightarrow ErSb_2 + (Sb)$	Eutectic		66.7	100	630	[7]
		~99	66.7	100	625	[8]
		99.4	66.7	100	620	[9]
		99	66.7	100	627	This work

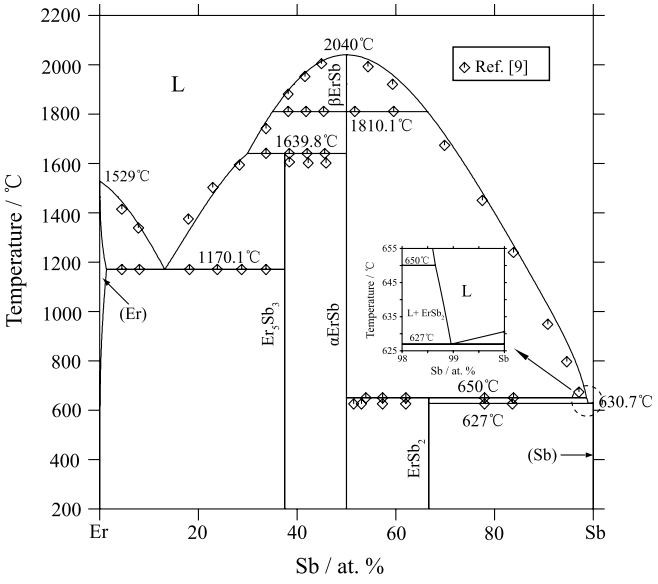

Fig. 3. Calculated phase diagram of the Er–Sb system compared with the experimental data [9].

4. Optimized results and discussion

The optimization of the thermodynamic parameters was carried out by using the PARROT program in the Thermo-Calc software [18], which can handle various kinds of experimental data. The experimental data of the phase diagram and thermodynamic properties were used as input to the program. Each piece of selected information was given a certain weight based on the importance of data, which was changed by trial and error during the assessment, until most of the selected experimental information was reproduced within the expected uncertainty limits.

4.1. The Er–Sb system

The calculated Er–Sb phase diagram compared with the experimental data is shown in Fig. 3, and the calculated compositions and temperatures for the invariant reactions compared with the selected experimental data are listed in Table 1. It is seen that the calculated results are in reasonable agreement with the experimental data [9]. The calculated maximum solid solubility of Sb in the hcp (Er) solution phase is 1.4 at%, which is in agreement with the experimental data (>1.0 at% Sb) [8,9] and considered reasonable. A set of complete self-consistent thermodynamic parameters describing the Gibbs free energy of each phase in the Er–Sb system is given in Table 2.

Table 2
Thermodynamic parameters in the Er–Sb system assessed in the present work.

Parameters in each phase (J/mol)
Liquid phase, format (Er, Sb)
${}^0L^{Liq}_{Er,Sb} = -211744 - 17.793T$,
${}^1L^{Liq}_{Er,Sb} = 41385 - 41.111T$,
${}^2L^{Liq}_{Er,Sb} = 48000 - 3.108T$
Hcp phase, format (Er, Sb)
${}^0L^{Hcp}_{Er,Sb} = -171000$
Er_5Sb_3 phase, format $(Er)_{0.625}(Sb)_{0.375}$
$\Delta^0G_f^{Er_5Sb_3} = -83050 + 1.23T$
$\alpha ErSb$ phase, format $(Er)_{0.5}(Sb)_{0.5}$
$\Delta^0G_f^{\alpha ErSb} = -111583 + 7.314T$
$\beta ErSb$ phase, format $(Er)_{0.5}(Sb)_{0.5}$
$\Delta^0G_f^{\beta ErSb} = -111266 + 7.162T$
$ErSb_2$ phase, format $(Er)_{0.333}(Sb)_{0.667}$
$\Delta^0G_f^{ErSb_2} = -75142 + 5.507T$

Table 3
Comparison of experimental and calculated values for the standard enthalpies of formation (kJ/mol of atoms) of intermetallic compounds in the Er–Sb system.

Phase	Experimental [11]	Experimental [10]	Calculated
Er_5Sb_3			−83.05
$\alpha ErSb$	−113.4	−109	−111.583
$ErSb_2$	−75.6		−75.142

The reference states of pure elements of Er and Sb are hcp and rhombohedral phases, respectively.

Table 4
Comparison of experimental and calculated values for the standard entropies of formation (J/K mol of atoms) of intermetallic compounds in the Er–Sb system.

Phase	Experimental [11]	Calculated
Er_5Sb_3		−1.23
$\alpha ErSb$	−7.6	−7.314
$ErSb_2$	−5.0	−5.507

The reference states of pure elements of Er and Sb are hcp and rhombohedral phases, respectively.

The calculated standard enthalpies of formation with reference states of the Er (hcp) and Sb (rhombohedral) phases compared with the experimental data are presented in Fig. 4 and Table 3, and a comparison of standard entropies of formation with reference states of the Er (hcp) and Sb (rhombohedral) phases between the calculated and the experimental data is shown in Fig. 5 and Table 4. It is seen that an agreement with the thermodynamic properties is obtained between the calculated results and the experimental

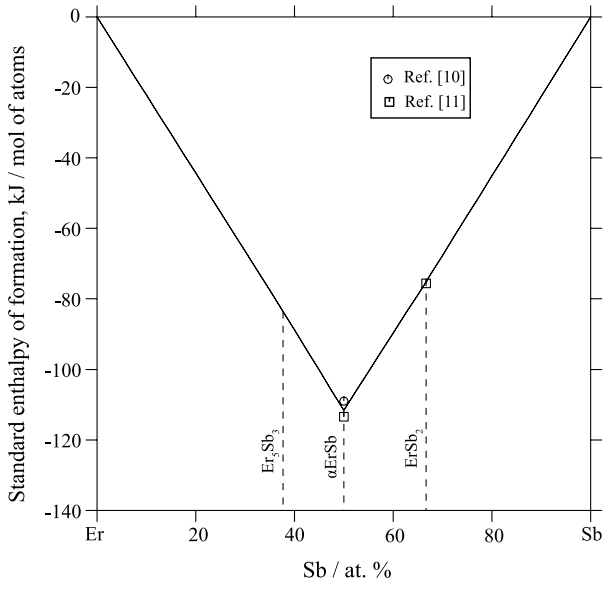

Fig. 4. Calculated standard enthalpies of formation with reference states of Er (hcp) and Sb (rhombohedral) phases in the Er–Sb system compared with the experimental data [10,11].

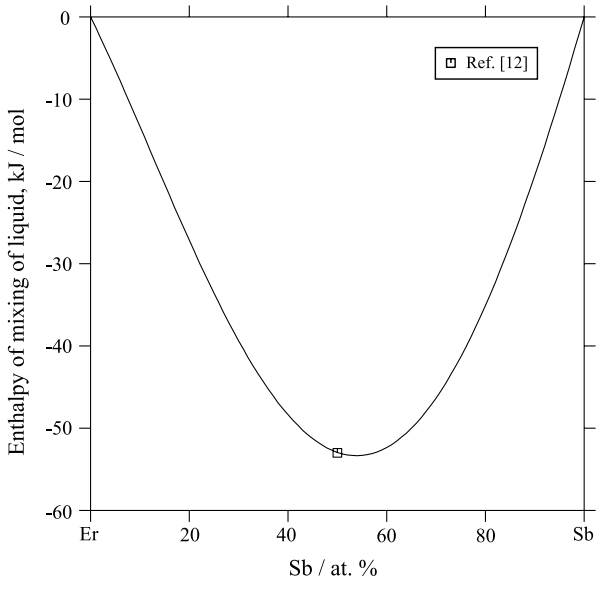

Fig. 6. Calculated enthalpies of mixing of liquid phase at 2100 °C with reference states of pure elements of Er (liquid) and Sb (liquid) compared with the predicted data [12].

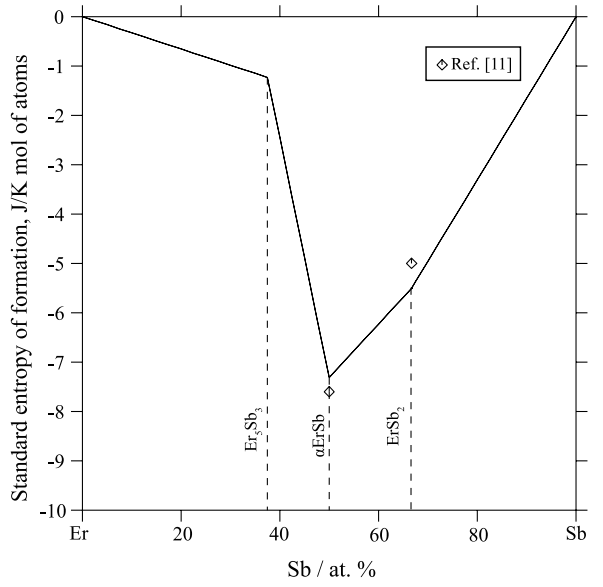

Fig. 5. Calculated standard entropies of formation with reference states of Er (hcp) and Sb (rhombohedral) phases in the Er–Sb system compared with the experimental data [11].

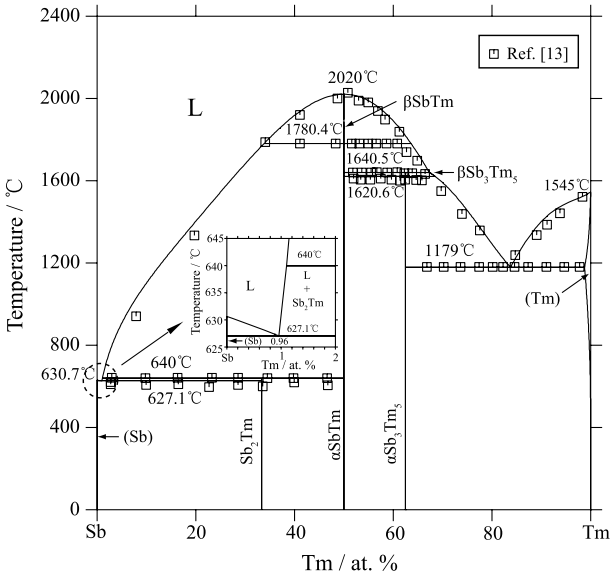

Fig. 7. Calculated phase diagram of the Sb–Tm system compared with the experimental data [13].

data. Fig. 6 shows the calculated enthalpies of mixing of the liquid phase at 2100 °C with reference states of pure Er (liquid) and Sb (liquid) in the Er–Sb binary system. The calculated value at 50 at% Sb is −52.936 kJ/mol, which is very close to the value of −53 kJ/mol predicted by Colinet et al. [12]. Therefore, the calculated enthalpies of mixing of the liquid phase in the Er–Sb system are reasonable.

4.2. The Sb–Tm system

The calculated Sb–Tm phase diagram compared with the experimental data is shown in Fig. 7, and the calculated compositions and temperatures for the invariant reactions compared with the selected experimental data are listed in Table 5. It is seen that the calculated results are basically in agreement with the experimental data of the phase equilibria [13], except for the temperature of eutectic reaction ($L \leftrightarrow Sb_2Tm + (Sb)$), which shows a discrepancy of 7.1 °C between the calculated results and the experimental data. A set of complete self-consistent thermodynamic parameters describing the Gibbs free energy of each phase in the Sb–Tm system is given in Table 6.

The calculated standard enthalpies of formation with reference states of the Sb (rhombohedral) and Tm (hcp) phases compared with the experimental data are presented in Fig. 8 and Table 7. It is seen that the calculated standard enthalpy of formation of the αSbTm phase is less negative than the value obtained by Pratt and Chua [10], but it is more negative than the value predicted by Colinet et al. [12]; furthermore, it is very close to the value predicted by Boer et al. [15]. By considering the agreement of the majority of the experimental data including the data of the phase equilibria and thermodynamic properties, we think that this calculated result can be accepted. Fig. 9 shows the calculated

Table 5
Experimental and calculated invariant reactions in the Sb–Tm system.

Invariant reaction	Reaction type	Composition (at.% Tm)			Temperature (°C)	Reference
$L \leftrightarrow (Sb) + Sb_2Tm$	Eutectic	<1.0	0	33.3	620	[13]
		0.96	0	33.3	627.1	This work
$L + \alpha SbTm \leftrightarrow Sb_2Tm$	Peritectic		50.0	66.7	640	[5,13]
		1.1	50.0	66.7	640	This work
$\alpha SbTm \leftrightarrow \beta SbTm$	Polymorphic		50.0		1780	[13]
			50.0		1780.4	This work
$L \leftrightarrow \beta SbTm$	Congruent		50.0		2020	[13]
			50.0		2020	This work
$L + \alpha SbTm \leftrightarrow \beta Sb_3Tm_5$	Peritectic		50.0	62.5	1640	[13]
		67.3	50.0	62.5	1640.5	This work
$\alpha Sb_3Tm_5 \leftrightarrow \beta Sb_3Tm_5$	Polymorphic		62.5		~1620	[13]
			62.5		1620.6	This work
$L \leftrightarrow \alpha Sb_3Tm_5 + (Tm)$	Eutectic	85	62.5	>98.5	1180	[13]
		83.8	62.5	98.8	1179	This work

Table 6
Thermodynamic parameters in the Sb–Tm system assessed in the present work.

Parameters in each phase (J/mol)
Liquid phase, format (Sb, Tm)
${}^0L^{Liq}_{sb,Tm} = -219000 - 32.067T$,
${}^1L^{Liq}_{sb,Tm} = -33941 + 49.848T$,
${}^2L^{Liq}_{sb,Tm} = 94097 - 12.3T$,
${}^3L^{Liq}_{sb,Tm} = -39081$
Hcp phase, format (Sb, Tm)
${}^0L^{Hcp}_{sb,Tm} = -185000$
Sb_2Tm phase, format $(Sb)_{0.667}(Tm)_{0.333}$
$\Delta^0G_f^{Sb_2Tm} = -76138 + 3.458T$
$\alpha SbTm$ phase, format $(Sb)_{0.5}(Tm)_{0.5}$
$\Delta^0G_f^{\alpha SbTm} = -112990 + 4.004T$
$\beta SbTm$ phase, format $(Sb)_{0.5}(Tm)_{0.5}$
$\Delta^0G_f^{\beta SbTm} = -112000 + 3.522T$
αSb_3Tm_5 phase, format $(Sb)_{0.375}(Tm)_{0.625}$
$\Delta^0G_f^{\alpha Sb_3Tm_5} = -83519 - 2.621T$
βSb_3Tm_5 phase, format $(Sb)_{0.375}(Tm)_{0.625}$
$\Delta^0G_f^{\beta Sb_3Tm_5} = -82824 - 2.988T$

Table 7
Comparison of experimental and calculated values for the standard enthalpies of formation (kJ/mol of atoms) of intermetallic compounds in the Sb–Tm system.

Phase	Predicted [12]	Experimental [10]	Experimental [15]	Calculated
Sb_2Tm	−71			−76.138
$\alpha SbTm$	−88	−157	−115	−112.99
αSb_3Tm_5	−80			−83.519

The reference states of pure elements of Sb and Tm are rhombohedral and hcp phases, respectively.

enthalpies of mixing of the liquid phase at 2200 °C with reference states of pure Sb (liquid) and Tm (liquid) in the Sb–Tm binary system. The calculated value at 50 at% Tm is −54.75 kJ/mol, which is close to −52 kJ/mol predicted by Colinet et al. [12]. Therefore, the calculated enthalpies of mixing of the liquid phase in the Sb–Tm system are reasonable.

5. Conclusions

The phase diagrams in the Er–Sb and Sb–Tm binary systems were thermodynamically assessed based on experimental data including phase equilibria and thermodynamic data, and most of the experimental information can be satisfactorily reproduced on the basis of the optimized thermodynamic parameters.

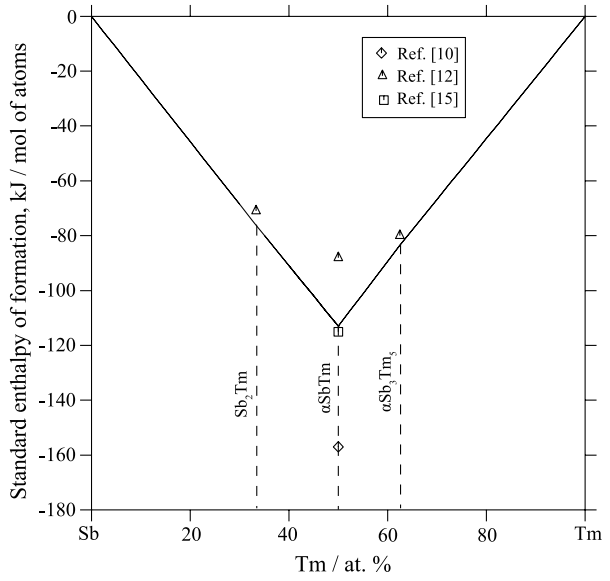

Fig. 8. Calculated standard enthalpies of formation with reference states of Sb (rhombohedral) and Tm (hcp) phases in the Sb–Tm system compared with the predicted data [10,12,15].

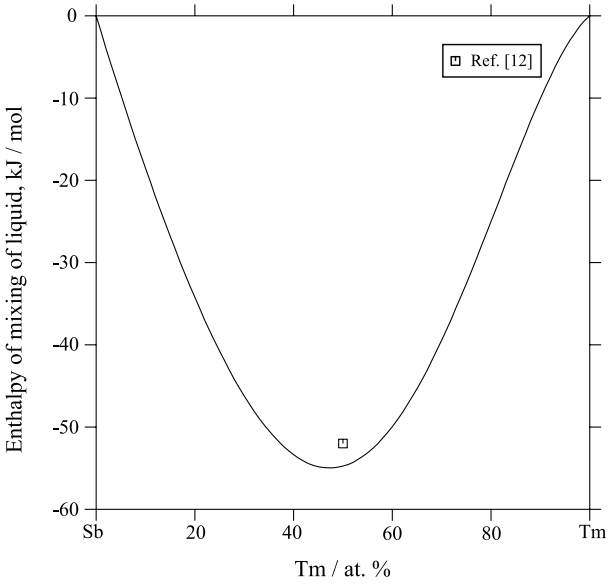

Fig. 9. Calculated enthalpies of mixing of liquid phase at 2200 °C with reference states of pure elements of Sb (liquid) and Tm (liquid) compared with the predicted data [12].

Acknowledgments

This work was supported by the National Natural Science Foundation of China (Grant No. 51031003), the Ministry of Education of China (Grant No. 707037) and the Ministry of Science and Technology of China (Grant Nos. 2009DFA52170 and 2009AA03Z101). Feng Gao is also grateful for support from the Doctoral Foundation of Qingdao University of Science and Technology.

Appendix. Supplementary data

Supplementary material related to this article can be found online at doi:10.1016/j.calphad.2011.08.001.

References

[1] B.L. Mordike, T. Ebert, Mater. Sci. Eng. A 302 (1) (2001) 37–45.
[2] P. Bakke, H. Westengen, JOM 56 (11) (2004) 191.
[3] J. Chao-Chi, K. Chun-Hao, Mater. Trans. 48 (2007) 265.
[4] G.Y. Zhang, H. Zhang, D. Wei, Z.C. Luo, Y.C. Li, Acta Phys. Sin. 58 (1) (2009) 444–449.
[5] M.N. Abdusalyamova, O.R. Burnashev, K.E. Mironov, O.I. Rakhmatov, N.D. Fazlyeva, Izv. Akad. Nauk SSSR, Neorg. Mater. 24 (3) (1988) 495–498 (in Russian); TR: Inorg. Mater. 24 (3) (1988) 409–411.
[6] M.N. Abdusalyamova, J. Alloy. Comp. 202 (1993) L15–L20.
[7] H. Okamoto, J. Phase Equilibria. 16 (3) (1995) 283.
[8] M.N. Abdusalyamova, O.I. Rakhmatov, J. Alloy. Comp. 299 (2000) L1–L3.
[9] M.N. Abdusalyamova, O.I. Rakhmatov, Z. Naturforsch 57a (2002) 98–100.
[10] J.N. Pratt, K.S. Chua, Final report 2027/048/RL, Department of Physical Metallurgy and Science of Materials, University of Birmingham, UK, 1970.
[11] V.I. Goryacheva, Ya.I. Gerasimov, V.P. Vasilev, Zh. Fiz. Khim 55 (1981) 1080–1082.
[12] C. Colinet, A. Pasturel, A. Percheron-Guégan, J.C. Achard, J. Less-Common. Met. 102 (1984) 239–249.
[13] M.N. Abdusalyamova, O.I. Rakhmatov, N.D. Fazlyeva, A.G. Chuiko, Izv. Akad. Nauk SSSR, Neorg. Mater. 27 (8) (1991) 1650–1652 (in Russian); TR: Inorg. Mater. 27 (8) (1991) 1386–1388.
[14] H. Okamoto, J. Phase Equilibria. 15 (3) (1994) 370.
[15] F.R. Boer, R. Boom, W.C.M. Mattens, A.R. Miedema, A.K. Niessen, Cohesion in metals, in: Transition Metal Alloys, North-Holland, Amsterdam, 1988.
[16] A.T. Dinsdale, CALPHAD 15 (1991) 317–425.
[17] O. Redlich, A.T. Kister, Ind. Eng. Chem. 40 (1948) 345–348.
[18] B. Sundman, B. Jansson, J.O. Andersson, CALPHAD 9 (1985) 153–190.